KLF5 Inhibition Overcomes Oxaliplatin Resistance In Patient-Derived Colorectal Cancer Organoids by Restoring Apoptotic Response

Xiaohui Shen
Shanghai Jiao Tong University School of Medicine
Han Gao
Shanghai Jiao Tong University School of Medicine
Yuchen Zhang
Shanghai Jiao Tong University School of Medicine
Zhuoqing Xu
Shanghai Jiao Tong University School of Medicine
Wenqing Feng
Shanghai Jiao Tong University School of Medicine
Wenchang Li
Shanghai Jiao Tong University School of Medicine
Yiming Miao
Shanghai Jiao Tong University School of Medicine
Zifeng Xu
Shanghai Jiao Tong University School of Medicine
Yaping Zong
Shanghai Jiao Tong University School of Medicine
Jingkun Zhao
Shanghai Jiao Tong University School of Medicine
Aiguo Lu (luaiguo1965@163.com)
Shanghai Jiao Tong University School of Medicine

Research

Keywords: Colorectal cancer, organoid, oxaliplatin., ML264, drug resistance

Posted Date: December 22nd, 2020

DOI: https://doi.org/10.21203/rs.3.rs-130881/v1

Version of Record: A version of this preprint was published at Cell Death & Disease on April 1st, 2022. See the published version at https://doi.org/10.1038/s41419-022-04773-1.

Abstract

Background: Oxaliplatin resistance is a major challenge for treatment of metastatic colorectal cancer (mCRC). Many molecular targeted drugs for refractory CRC have been developed to solve colorectal cancer drug resistance, but their effectiveness and roles in the progression of CRC and oxaliplatin-resistance still not clear.

Methods: PDOs derived from CRC patients were constructed to conduct the sensitivity assays of oxaliplatin in vitro. Oxaliplatin resistant PDOs were selected and treated under the combined treatment of ML264(a KLF5 inhibitor) and oxaliplatin to determine the effects of KLF5 inhibition on apoptosis. Using CRC cell lines to investigate downstream mechanisms and xenograft models to confirm whether ML264 can restore oxaliplatin sensitivity of CRC cells in vivo.

Results: We successfully constructed CRC PDOs and conducted the sensitivity test of oxaliplatin in PDOs from different patients. We found that ML264 restores oxaliplatin sensitivity in CRC PDOs by restoring the apoptotic response, and this effect was achieved by inhibiting the KLF5/Bcl-2/caspase3 signal pathway. Chromatin immunoprecipitation (ChIP) and luciferase reporter assay verified that KLF5 promoted the transcription of Bcl-2 in CRC cells. KLF5 inhibition also overcomed oxaliplatin resistance in xenograft tumors.

Conclusions: Our study demonstrated that ML264 can restores oxaliplatin sensitivity in CRC PDOs by restoring the apoptotic response. KLF5 might be a potential therapeutic target for CRC resistant to oxaliplatin. PDOs have strong potential in evaluating inhibitors and drug combinations therapy in a preclinical environment.

Background

Cancer is developing into one of the main causes of death worldwide. Colorectal cancer (CRC) is one of the most common types of malignant tumors of the digestive system[1]. Although many advances have been made in the diagnosis and treatment of CRC, the mortality rate associated with CRC is still high[2]. The classical treatments for colorectal cancer include surgical resection, chemotherapy and radiation. However, when curative surgery is impossible, chemotherapy represented by oxaliplatin may initially reduce the size of the tumor, but tumor recurrence or metastasis is almost inevitable[3]. Cancer stem cells (CSC) are considered to be associated with this phenomenon, which can promote growth, mediate anticancer drugs/radiation resistance and seed metastasis[4]. "Modern" molecular targeted therapy for (metastatic) CRC is considered to be one of the effective ways to solve colorectal cancer drugs resistance, which is also the focus of current oncology research[5, 6].

Organoids are micro-organs with three-dimensional structures formed by stem cells under special culture conditions in vitro[7]. They reproduce the structure and function of corresponding organs in vivo in many aspects. More than 30 years ago, Mina Bissell[8] reported the technique of culturing functional breast epithelium in three-dimensional matrices, and this universal technology has led to the establishment of

many human organ models in vitro. In addition to being used to establish normal organ models in vitro, organoids are often used to study tumorigenesis. At present, patient–derived organoids (PDOs) have been established from various carcinomas, for example, for gastric[9], colorectal[10],pancreatic[11]、breast[12], and ovarian cancers[13]. PDOs represents a model system that can be compared with current tumor models including genetically engineered mouse models, tumor cell lines, and primary patient-derived tumor xenografts (PDXs)[14].

Kruppel-like factor 5 (KLF5), a stem-related transcription factor, is preferentially expressed in embryonic stem cells or cancer stem cells. KLF5 plays an important role in tumor cells proliferation, survival, apoptosis and drug sensitivity[15]. The drug resistance of tumor cells or tumor stem cells may be related to their ability to adaptively reprogram in response to drug treatment. Previous studies have suggested that KLF5 may be involved in this process[16, 17].

In this study, we employed PDO models to further explore potential molecular mechanisms of oxaliplatin resistance in colorectal cancer, including testing the efficiency of combination therapy of oxaliplatin and ML264(the KLF5 inhibitor)[18]. We first successfully constructed PDOs derived from tumor tissues of CRC patients in vitro, and conducted the sensitivity test of oxaliplatin in PDOs from different patients. In addition, we found that the sensitivity of CRC organoids to oxaliplatin is negatively correlated with the expression of KLF5, and KLF5 can inhibit the apoptosis of CRC cells induced by oxaliplatin. Finally, we confirmed that KLF5 inhibitor ML264 can enhance the efficiency of oxaliplatin therapy in CRC in vivo and vitro models. These findings indicate that KLF5 participates in the resistance mechanism of CRC to oxaliplatin through inhibiting cell apoptosis. In addition, our study shows the strong potential of PDOs in evaluating inhibitors and drug combinations therapy in a preclinical environment.

Methods

Patients and specimens

The specimens of 12 patients were collected after obtaining the informed consent from the Biomedical Ethics Committee of Ruijin Hospital (Table 1). All these patients were diagnosed as CRC pathologically and accepted laparoscopic surgery in Minimally Invasive Surgery Centre, Ruijin Hospital, Shanghai Jiaotong University.

Specimens processing and tumor cell preparation

Surgical specimens were washed with PBS containing penicillin-streptomycin solution and minced into meat emulsion using tweezers and disposable surgical blades. Tissue fragments were transferred to a 50ml centrifuge tube, and digested with 0.5mg/ml type IV collagenase in DMEM at 37°C for 1 hour until fully digested. The digested tissue suspension was filtered through 500 μm and 100 μm cell strainers in sequence to remove residual tissue. Then the filtrate was re-filtered through a 40μm cell strainer, and the cell clusters retained in the strainer were collected and washed twice with PBS. Cell clusters were transferred to the stem cell culture medium (DMEM/F12 medium with glutamine, non-essential amino

acids, 8 ng/mL bFGF, 2-mercaptoethanol, serum substitute and penicillin-streptomycin solution) and cultured at 37°C, 5% CO2 and 20% O2. After 24 hours of cultivation, organoids with obvious spherical structures and smooth surfaces are formed.

The cultivation and expansion of PDOs

Once PDOs were formed, added the growth factors required for CRC organoid culture in the stem cell medium, including 50 ng/mL EGF, 1μg/ml R-Spondin1, 500 nM A8301, 50 ng/mL Noggin, 3 μM SB202190, 10 nM prostaglandin E2, 1 x B27, 10 mM nicotinamide. A 23-gauge needle was used to tear the PDO for expansion. For 3D culture, PDOs were embedded in Cellmatrix type I-A (Nitta gelatin) and overlaid with organoid culture medium. 0.2 mg/mL type 4 collagenase was used to digest Cellmatrix to release PDOs.

Flow cytometry analysis

PDOs were collected and washed with PBS, and digested into single cell suspension using 0.25% trypsin/EDTA. The cells were washed with PBS, and then incubated with fluorescent-conjugated primary antibodies in PBS containing 0.5% BSA at 4°C in the dark for 30 min. Antibodies used including EpCAM, CEA CAM1, CD31 and CD45. More information about the antibody was listed in Table S1. Samples were detected using flow cytometry (BD Biosciences) and analyzed by FlowJo software (Tree Star).

Histological staining

Tissues and PDOs were fixed in 4% neutral buffered formalin and embedded in paraffin. H&E staining and immunohistochemical staining were performed on the slices. Antibodies of IHC analysis included Ki-67, EpCAM, MUC2, α-SMA, CD68. More information about the antibody was listed in Table S2. TUNEL apoptosis detection kit was used according to the manufacturer's instructions. Positive cells were scored irrespective of the intensity of staining. The percentage of positive cells was scored semi-quantitatively by two independent individuals.

Immunofluorescence assays and confocal microscopy

Immunofluorescence assays were performed as previously described[19]. PDOs were collected and fixed with 4% paraformaldehyde for 15 min. After washing with PBS, PDOs were permeabilized with 0.1% Triton X-100 at room temperature for 5 min. Then PDOs were washed with PBS and blocked with 5% BSA for 1 hour at room temperature. PDOs were incubated with primary antibodies overnight at 4°C, including E-Cadherin, β-catenin, Ki-67 and EpCAM. Details of the antibody were listed in Table S3. After that, PDOs were washed and incubated with Alexa Fluor 488 or Alexa Fluor 555 Secondary Antibody (Abcam) at 37°C for 2 hours. After washing with PBS, diamidino phenylindole (DAPI, Santa Cruz, USA) was used to counterstain the nucleus. The results were visualized using a laser scanning confocal microscope (Zeiss, LSM510).

Apoptosis detection

Flow cytometric assays of apoptosis were performed as previously described[20]. Annexin V-FITC Apoptosis Detection Kit (BD Pharmingen) was used to detect cell surface Annexin V expression and propidium iodide (PI) uptake by flow cytometry. Cells were collected, washed twice with ice-cold PBS, and suspended in 100 µl binding buffer. Using 3 µl Annexin V-FITC and 5 µl PI to stain cells in the dark at room temperature for 15 minutes. Apoptosis was analyzed by flow cytometry using the FACSCalibur system (BD Biosciences, USA). According to the manufacturer's instructions, using TUNEL Apoptosis Detection Kit (Beyotime) to stain PDOs, and detecting apoptosis by fluorescence microscope. GreenNuc™ Caspase-3 Assay Kit (Beyotime) was used to detect Caspase-3/7 activity in PDOs according to the manufacturer's instructions. Using Ac-DEVD-CHO, a reversible inhibitor of Caspase-3/7, as a negative control. The results were visualized by fluorescence microscope.

Animal research

Four-week-old male BALB/c nude mice were purchased from the Shanghai Institute of Zoology, Chinese Academy of Sciences. All experiments were performed in accordance with the official recommendations of the Chinese Zoological Society, and animals were cared for humanity in accordance with the standards outlined in the "Guidelines for the Care and Use of Laboratory Animals". PDOs were injected subcutaneously in the flanks of nude mice. Mice were observed for up to 3 months and killed when tumor diameter reaches 10 mm. For drug treatment, when tumors reached about 5mm in diameter, all mice were randomly divided into four groups (3 in each group, Group 1: Vehicle-only solution; Group 2: ML264 25mg/kg; Group 3: oxaliplatin 5 mg/kg; Group 4: oxaliplatin 5 mg/kg +ML264 25mg/kg. These compounds are dissolved in NS (physiological saline solution) and administered intraperitoneally (ip). The dosing regimen is: oxaliplatin once a week, ML264 twice a week, each treatment regimen lasting for a duration of 14 days. Use a vernier caliper to measure the tumor size and record the data twice a week. Three days after the last injection, the animals were sacrificed by cervical decapitation, and tumors were excised and retained for further analyses. Samples were prepared for Western blot analysis and histological staining.

Evaluation of PDOs growth

The evaluation of PDOs growth was performed as previously described[21]. PDOs were evaluated after cultured in Cellmatrix type I-A for 1 week. The PDOs growth ratio was calculated as follows: (major axis length) × (minor axis length) after cultivation / (major axis length) × (minor axis length) before cultivation.

Drug sensitivity analysis

Stable growing CRC PDOs were used for drug sensitivity test. ~20 PDOs were embedded in Cellmatrix type I-A and plated in 96-well plates, and overlaid with organoid culture medium. PDOs were treated with oxaliplatin at 0, 0.25, 0.5, 1, 2 and 4µM respectively, and DMSO was added to the culture as a solvent control. The plate was incubated at 37°C, 5% CO2 for 7 days, and images were captured on days 1, 3, 5,

and 7 to evaluate PDOs growth and calculate growth ratio. Curve fitting of drug sensitivity data was conducted as mentioned[22], and the data was expressed as a percentage of growth starting from 0μM.

Cell lines

The human CRC cell lines used in our study were purchased from the American Type Culture Collection (ATCC, USA). All these cells were cultured in RPMI-1640 medium with 10% fetal bovine serum (FBS), penicillin (107 U/l), and streptomycin (10 mg/l) and incubated at 37 °C and 5% CO2.

RNA extraction and quantitative real-time PCR (qRT-PCR)

RNA extraction and qRT-PCR were performed as previously described[23]. Total RNA of PDOs was extracted using RNAprep pure Micro Kit (Tiangen, China) according to the manufacturer's instructions. Total RNA was reversed to cDNA using HiScript III RT SuperMix (Vazyme, China) and qPCR was performed using SYBR Green (Vazyme, China) according to the manufacturer's instructions. The primers of qPCR were purchased from Genewiz, China and the sequences were listed in Table S4. GAPDH was used as control. The relative expression ratio of mRNAs in each group was calculated by the $2^{-\Delta\Delta CT}$ method.

Protein extraction and Western blotting

Protein extraction and western blot analysis was performed as previously described[19]. Cells were collected at a 70-80% confluence, and total protein was extracted by RIPA (Solarbio, China) in the presence of Protease Inhibitor and Protein Phosphatase Inhibitor Cocktail (APExBIO, USA). The concentration of total protein lysate was quantified using BCA Protein Assay Kit (ThermoFisher, USA). Proteins were separated by SDS-PAGE and transferred to a PVDF membrane (Tanon, China). Antibodies of western blotting included KLF5, Cleaved Caspase-3, Caspase-3, Bcl-2, Bax and GAPDH. Details of the antibody were listed in Table S5. Goat anti-rabbit or goat anti-mouse HRP-conjugated IgG was used as the secondary antibody (proteintech, USA), and samples were incubated at room temperature for 2 h. The ECL chemiluminescence agent (Millipore, USA) was used to visualize the membrane. The image was captured by Tanon Chemiluminescence Imaging System (Tanon, China). GAPDH was used as the internal control.

siRNA knockdown

CRC cells were transiently transfected with BCL2 or Bax siRNA (TSINGKE, China) using Lipo3000 (Invitrogen) according to the manufacturer’s instructions. Western blot was used to test the downregulation efficiency of siRNA. The targeting site sequences were listed in Table S6.

Chromatin immunoprecipitation (ChIP)

ChIP assays were performed as previously described[24]. SimpleChIP® Plus Enzymatic Chromatin IP Kit (CST, USA) was used according to the manufacturer’s instructions. The presence of predicted

transcription factor binding regions pulled by antibodies was examined by qPCR. The primers of qPCR were purchased from Genewiz, China and the sequences were listed in Table S4.

Luciferase reporter assay

Luciferase reporter assay was performed as previously described[25]. The BCL2 promoter was cloned into the pGL3-Basic luciferase plasmid (Promega, Madison, USA) to construct WT BCL2 reporter. BCL2 truncat plasmid and mutant plasmid were also constructed（Fig. 5E, H）. For Renilla luciferase reporter assay, each reporter construct was co-transfected into HEK293T cells together with KLF5 plasmid or Control plasmid. After 48 h of incubation, luciferase activities were measured using the Dual luciferase Reporter Assay System (Promega).

Statistics

All of the statistical analysis were performed by SPSS 20.0 software or R software 3.1.2 (R Core Team). Quantitative variables were analyzed by Student's t-test. Data were shown in mean ± SD. All experiments were performed in triplicate. A two-tailed value of $P < 0.05$ was considered statistically significant.

Results

Generation of patient-derived organoids from colorectal cancer

CRC PDOs were established as previously described[10,21]. We collected 18 tissue specimens from 12 CRC patients, including 12 tumor tissue specimens and 6 adjacent normal tissue specimens. Of the total 18 included samples, all normal tissue samples (n=6) were unable to form PDOs in our culture system (Fig. 1A). For 12 tumor samples, 1 sample had bacterial infection, and 2 samples failed due to too few tumor cells or low proliferation rate(Table 1). Overall, we obtained a PDO culture success rate of approximately 75% (9 of 12 cases), which is consistent with previous reports[26].

Characteristics of patient derived CRC organoids

Patient derived CRC organoids were spherical and bright with a smooth surface (Fig. 1A). The diameter of PDOs was about 40-1000μm. A PDO with a diameter of 100μm was consisted of about 100 cells. CRC PDOs can proliferate stably in suspension culture or 3D culture (Fig. 1B). Since tumor tissue contains heterogeneous cellular components, we used flow cytometry to analyze the composition and purity of cells in CRC PDOs. The tested cells included the following three groups: group 1 was the flow-through(FT), which passed through the 40μm filter when extracting PDOs; group 2 was the cell mass (PDO Day 1), which remained in the 40μm filter when extracting PDOs; group 2 was the PDOs after 10 days of culture (PDO Day 10). The results revealed that besides EpCAM+ epithelial cells, FT also contained CD31+ endothelial cells and CD45+ blood cells. In contrast, PDOs hardly contained any CD45+ and CD31+ cells (Fig. 1C). In addition, when simultaneously labeling the expression of EpCAM and CEACAM in cells，it was found that compared with PDO Day 1 group，PDO Day 10 group only contained the EpCAM+/CEACAM+ cell population(Fig. 1D). The above results showed that the CRC PDOs we

constructed in vitro were highly purified cancer cell clusters. Next, we used immunodeficient mice to detect the tumor-initiating ability of CRC PDOs. As shown in the Fig. 1E, PDOs can form tumors in nude mice, indicating that PDOs contained tumorigenic cancer cells. E-cadherin–Mediated cell-to-cell contact is necessary for maintaining the spatial structure of PDOs and cancer cells survival[27]. Therefore, we detected the expression of E-cadherin in PDOs. The results of immunofluorescence showed that E-cadherin expression was located on the cell membrane of all cells in PDOs and linked by β-catenin (Fig. 1F). In addition, immunofluorescence assay simultaneously characterized the expression of epithelial cell marker EpCAM and tumor marker Ki-67 in PDOs (Fig. 1G).

PDOs retained the characteristics of the original tumor

Patient derived CRC organoids show the histological features of adenocarcinoma, including lumen structure and mucus production[10]. According to the differentiation level of the original tumor, CRC PDOs can show the histological features of highly differentiated adenocarcinoma cells with luminal structure, or of poorly differentiated adenocarcinoma cells without luminal structure(Fig. 2A). Immunohistochemical analysis was used to detect the expression of Ki-67, EpCAM, MUC2, α-SMA and CD68 in CRC PDOs and matched original tumors. The expression of Ki-67(a cell proliferation marker) and EpCAM(a epithelial cell marker) were retained in patient derived CRC organoids. In contrast, α-SMA, a marker of activated fibroblasts, and CD68, a macrophage marker, were detected in the microenvironment of the original tumor, but not in the PDOs(Fig. 2B). These results were consistent with previous reports[28].

Oxaliplatin Sensitivity Assay with Patient derived CRC organoids

We previously verified that CRC PDOs were composed of highly purified tumorigenic cells and retained the characteristics of parental tumors. Therefore, PDOs may be used for chemo-sensitivity assays in vitro. Oxaliplatin (a key drug widely used in clinical chemotherapy for colorectal cancer) were choosen to conduct drug sensitivity assays of PDOs from 6 CRC patients (table 1). All PDOs were exposed to oxaliplatin for 7 days, and each screen was repeated by two independent reviewers to determine inter-observer reliability. We calculated the growth ratio of PDOs after drug exposure and fitted dose-response curves. We found that the growth of CRC PDOs was inhibited in a dose-dependent manner by oxaliplatin, and the response of PDOs to oxaliplatin had individual differences (Fig. 2F). For example, in the PDOs derived from P1, the growth of PDOs was significantly inhibited at 2μM(Fig. 2C); in the PDOs derived from P2, the growth of PDOs was significantly inhibited at 1μM(Fig. 2D); whereas in PDOs derived from P4, even 4μM oxaliplatin was not enough to inhibit the growth of PDOs at the same level(Fig. 2E). These results suggested the potential of PDOs to detect individual chemical sensitivity of colorectal cancer.

ML264(a KLF5 inhibitor) restores oxaliplatin sensitivity in CRC PDOs by restoring the apoptotic response

To evaluate the cause of the growth inhibition of CRC PDOs induced by oxaliplatin, TUNEL Apoptosis Detection Kit was used to detect the level of apoptosis of PDOs. In the PDOs derived from P1, oxaliplatin significantly induced apoptosis in a dose-dependent manner (Fig. 3A, C). In addition, we detected the

expression of stemness-related transcription factor KLF5 in CRC PDOs. The results showed that as the dose of oxaliplatin treatment increased, the proportion of KLF5+ cells increased significantly (Fig. 3B, C). These data indicated that KLF5 may be involved in the apoptosis process induced by oxaliplatin. Next, we investigated if KLF5 inhibitor ML264 can be used to restore oxaliplatin sensitivity in CRC PDOs. Oxaliplatin resistant PDOs (P4 and P6) were selected for drug sensitivity assays that under the combined treatment of ML264 and oxaliplatin. We found that ML264 significantly reduced the dose of oxaliplatin required to inhibit the growth of PDOs (Fig. 3D, E). The analysis of the apoptosis level of CRC PDOs showed that even 4μM oxaliplatin could not induce significantly apoptosis in oxaliplatin resistant PDOs (Fig. 3F). However, treating with oxaliplatin combined with ML264 significantly restored the apoptosis of PDOs derived from P4 and P6 (Fig. 3G, H, I). In addition, the activity of caspase 3 was also significantly increased in PDOs when treating with oxaliplatin combined with ML264(Fig. 3J, K). These results indicated that the KLF5 inhibitor ML264 can restore the apoptotic response and then enhance the oxaliplatin sensitivity of CRC PDOs.

The KLF5/Bcl-2/caspase3 signal pathway affects oxaliplatin-induced apoptosis of CRC cells

Previous researches have reported many molecules involved in drug-induced apoptosis, including caspase family, Bcl family, PARP1, BIRC5 and TNF[29-33]. To further investigate the underlying molecular mechanism, oxaliplatin resistant PDOs were divided into four groups (Group 1: Control; Group 2: ML264 0.5μM; Group 3: oxaliplatin 1μM; Group 4: oxaliplatin 1μM +ML264 0.5μM). Then, qPCR and Western blotting were used to detect the expression of apoptosis-related molecules. The results of qPCR showed that at the RNA level, oxaliplatin significantly induced the expression of Bcl-2 and Bax, whereas in oxaliplatin + ML264 treated group, the expression of Bcl-2 was inhibited while the expression of Bax and CASP3 increased (Fig. 4A). Similarly, Western blot revealed that after treated with oxaliplatin combined with ML264, the expression of anti-apoptotic molecule Bcl-2 decreased, while the expression of pro-apoptotic Bax and Cleaved Caspase-3 increased (Fig. 4B, C).

Next, CRC cell lines were used to further explore the downstream molecular signaling pathways of KLF5. We generated stably transfected CRC cell lines, including RKO control(RKO/Vector), RKO with KLF5 over-expression(RKO/KLF5), SW620 control(SW620/sh-NC) and SW620 with KLF5 down-regulation (SW620/sh-KLF5). To evaluate the role of KLF5 in oxaliplatin-induced apoptosis in CRC cells, flow cytometry was used to detect the level of apoptosis with or without oxaliplatin treatment. Compared with the control group, high expression of KLF5(RKO/KLF5) significantly suppressed cell apoptosis, while low expression of KLF5(SW620/sh-KLF5) significantly promoted cell apoptosis. In particular, when treated with 1 μM oxaliplatin, the anti-apoptotic effect mediated by KLF5 was significantly enhanced in CRC cells (Fig. 4D). Similarly, we used qPCR and Western blotting to detect the expression of apoptosis-related molecules in stably transfected CRC cell lines. The results of qPCR showed that KLF5 significantly induced the expression of Bcl-2 but inhibited the expression of Bax and CASP3(Fig. 4E). At the protein level, KLF5 also promoted the expression of Bcl-2 and inhibited the expression of Bax (Fig. 4F). Although KLF5 cannot regulate the expression of Caspase-3 at the protein level, it significantly suppressed the

expression of Cleaved Caspase-3, which directly acted as an effector of caspase 3 to participate in the apoptotic response[34].

Small interfering RNA technology was used to knock down Bcl-2 and Bax in CRC cells to investigate which pathways mediate KLF5-related cell apoptosis. We have confirmed that KLF5 significantly induced the expression of Bcl-2, so we first knocked down Bcl-2 in KLF5 highly expressed cells (RKO/KLF5 and SW620/sh-NC). The results showed that knocking down Bcl-2 did not affect the expression of Bax, but significantly promoted the expression of Cleaved Caspase-3. Similarly, according to our previous results, KLF5 suppressed the expression of Bax. We next chose KLF5 weakly expressed cells (RKO/Vector and SW620/sh-KLF5) to knock down Bax, and found that knocking down Bax did not affect the expression of Bcl-2 or Cleaved Caspase-3(Fig. 5A, B). We further confirm whether Bcl-2 was the main executor in KLF5 mediating anti-apoptosis response. The results of Western blotting showed that inhibiting the expression of Bcl-2 can reverse the function of KLF5 to inhibit apoptosis. On the contrary, inhibiting the expression of Bax cannot reverse the function of KLF5 in anti-apoptosis (Fig. 5C, D). These results suggested that the effect of KLF5 on inhibiting cell apoptosis was mainly implemented by Bcl-2 and its downstream molecular caspase 3.

KLF5 promotes the transcription of Bcl-2 in CRC cells

Because KLF5 can directly bind to the promoter region of target genes and regulate transcription and expression of downstream genes[35], we further explore the mechanism in KLF5-induced Bcl-2 gene transcription. We first predicted three KLF5-binding elements (KBE1 to KBE3) on Bcl-2 promoter region by JASPAR software (Fig. 5E). Then, the plasmids of the full-length of Bcl-2 promoter region(pGL3-Bcl2-FL) and two truncated Bcl-2 promoter fragments (truncated 1: -300 to +100 nt, truncated 2: -100 to +100 nt) were constructed (Fig. 5E). The pGL3-basic was used as a negative control. Luciferase reporter assay was used to detect the transcriptional regulation level of KLF5 on the luciferase plasmid we constructed. The results showed that overexpression of KLF5 promoted the luciferase activity of pGL3-Bcl2-FL. In contrast, in truncated 1 and truncated 2 plasmids, which did not contain KBE1 sequence, KLF5 overexpression had no significant effect on luciferase activity (Fig. 5G). In addition, the sequence of KBE1 and KBE2 were deleted from the full-length of Bcl-2 promoter plasmid (Bcl-2 WT) to construct Bcl-2 Mut 1 and Bcl-2 Mut 2 plasmids (Fig. 5H). Expectedly, the mutation of KBE1 could significantly reduce the activation of the Bcl-2 promoter (Fig. 5I). Subsequently, we designed a PCR primer for Bcl-2 promoter region based on the results of Luciferase reporter assay. Chromatin immunoprecipitation (ChIP) verified the direct binding of KLF5 to the predicted site(KBE1) of the Bcl-2 promoter (Fig. 5F). These results suggested that the effective KLF5-binding site on Bcl2 promoter was between -433 and -424 nt (KBE1).

Inhibition of KLF5 overcomes oxaliplatin resistance in xenograft tumors

We compared the effects of oxaliplatin or oxaliplatin combined with ML264 on established CRC xenograft tumors in nude mice to determine whether KLF5 inhibition can restore oxaliplatin sensitivity in vivo. The results showed that in xenograft tumors derived from oxaliplatin-resistant PDOs, the combined use of ML264 can significantly inhibit tumor growth (Fig. 6A, B, C). TUNEL and ki-67 immunostaining

showed that compared with control group and the oxaliplatin single-treatment group, ML264 significantly restored the oxaliplatin-induced tumor apoptosis (Fig. 6D). Western blot conducted that in oxaliplatin-resistant xenografts, oxaliplatin treatment significantly promoted the expression of KLF5 and Bcl-2. However, the combined treatment of ML264 and oxaliplatin, the expression of KLF5 and Bcl-2 was inhibited and the expression of Cleaved Caspase-3 was promoted (Fig. 6E).

Discussion

In the clinical treatment of colorectal cancer, systemic treatment (neoadjuvant or adjuvant cytotoxic chemotherapy) is often used in combination with surgical treatment[36]. But for many CRC patients, especially metastatic CRC patients, this method only brings a moderate benefit in terms of survival[37]. They are either inherently insensitive to chemotherapy or develop resistance during treatment[38]. Therefore, developing more effective treatment methods to solve the problem of drug resistance of existing therapies are urgently needed. In the development of novel anticancer therapies, predictive vitro models to help match patients to treatments are highly needed. Chemotherapy and targeted drugs can be first used in these models to test the safety and effectiveness instead of be used directly in patients[39]. In this study, we successfully constructed an organoid model derived from CRC according to previous reports, and our success rate of PDOs cultured was about 75%(9 out of 12 cases).

The characteristics of PDOs include the following aspects: PDOs can be effectively derived from tumor tissues of patients and can be xenotransplanted; faithful response and maintain the characteristics of parental tumors, with individual differences; tumor PDOs can reliably reflect the response of corresponding patients to the same drug[40]. We identified CRC organoids we constructed according to the characteristics of PDOs. The results showed that CRC PDOs were composed of highly puritied colorectal cancer cells without other cellular components. PDOs can form tumors in nude mice, indicating that PDOs contained oncogenic cancer cells. In addition, CRC PDOs retained the characteristics of the original tumor, including the similarity of histology and the consistency of protein expression. We further tested the ability of PDOs to mimic the response of chemotherapy in patients. Oxaliplatin sensitivity assay showed that the response of PDOs to oxaliplatin had individual differences, suggesting the potential of PDOs to detect individual chemical sensitivity of colorectal cancer.

Except for the personalized testing of chemotherapy and targeted therapy, PDOs are also suitable for high-throughput drug screening[41]. In particular, PDOs can test various drug combinations in vitro to generate new treatments, which may help us understand the potential molecular mechanisms of tumor resistance[42]. We used CRC PDOs to test the effect of a small molecule inhibitor ML264 in the oxaliplatin treatment of colorectal cancer. The results showed that ML264 can restore the oxaliplatin sensitivity in CRC PDO, indicating that inhibition of KLF5 is an effective approach to resensitize CRC with oxaliplatin resistance. The resistance of malignant tumors to chemotherapy is mostly mediated by anti-apoptotic effects[43]. Therefore, we suspected that KLF5 was involved in the process of oxaliplatin-induced apoptosis in colorectal cancer. The results of apoptosis detection showed that in oxaliplatin-sensitive CRC PDO, oxaliplatin significantly induced apoptosis in a dose-dependent manner. In contrast, in

oxaliplatin resistant CRC PDO, oxaliplatin can not induce apoptosis. Interestingly, oxaliplatin also significantly induced the expression of KLF5 in CRC cells. Inhibition of KLF5 can restore the apoptotic response of CRC cells, and then enhance the oxaliplatin sensitivity of CRC PDO. Similarly, the treatments of CRC xenograft tumors proved that inhibition of KLF5 can overcome oxaliplatin resistance in vivo.

Previous researches have reported many molecules involved in drug-induced apoptosis [44], we screened some of these molecules to detect whether they are affected by oxaliplatin and ML264. The results showed that oxaliplatin significantly induced the expression of Bcl-2 and Bax, while the combined treatment of oxaliplatin and ML264 inhibited the expression of Bcl-2 and promoted the expression of Bax and CASP3. Using small interfering RNA knockdown technology, we further confirmed that KLF5 inhibitor ML264 affected oxaliplatin-induced CRC apoptosis by inhibiting the Bcl-2/caspase3 signaling pathway. The results of Luciferase reporter assay and ChIP showed that KLF5 promoted the expression of Bcl-2 through transcriptional regulation, thereby exerting its anti-apoptotic function.

In summary, our study provides reliable laboratory evidence that KLF5 is an attractive therapeutic target for CRC, especially CRC resistant to oxaliplatin. At the same time, we also provide a new idea for future anti-tumor drug resistance studies. That is, using patient derived organoids for drug combination screening, then conduct further researches on potential mechanisms based on the target of effective drugs. However, relying too much on the examination results of tumor organoids also brings certain risks. Although a large number of biobanking researches have confirmed that PDOs reflect the characteristics of primary tumors at the macroscopic DNA sequence level[10]. It is not clear whether PDOs can reflect intratumoral heterogeneity, which may cause the heterogeneity of the response of PDOs to the drug, and interfere with researcher's judgment[42]. Therefore, more clinical trials are needed to measure the sensitivity and specificity of PDOs to patients receiving drug treatment. In conclusion, tumor organoids can fill the gap between cancer research and clinical trials, and act as a promising tool model for future scientific research and clinical treatment.

Conclusion

In conclusion, this study reveal that overexpression of KLF5 and its downstream anti-apoptotic factor Bcl-2 was one of the mechanisms for CRC to resist oxaliplatin. The combined treatment of KLF5 inhibitor ML264 can reverse the oxaliplatin resistance of CRC by restoring apoptotic response through inhibiting the KLF5/Bcl-2/caspase3 signal pathway (Fig. 7). These findings support that KLF5 inhibition may be a promising option of targeted therapy for oxaliplatin resistant colorectal cancer. In addition, our study shows the strong potential of PDOs in evaluating inhibitors and drug combinations therapy in a preclinical environment. However, we demonstrated the conclusion only using PDOs and CRC cell lines in vivo and in vitro, there are still some limits of our research. The effect of KLF5 on oxaliplatin resistance remains to be studied further.

Abbreviations

CRC, colorectal cancer; ChIP, Chromatin immunoprecipitation; CSC, Cancer stem cells; PDOs, patient derived organoids; PDXs, patient-derived tumor xenografts; KLF5, Kruppel-like factor 5; DAPI, diamidino phenylindole; PI, propidium iodide; ip, intraperitoneally; FBS, fetal bovine serum; FT, flow-through; KBE, KLF5-binding elements;

Declarations

Ethics approval and consent to participate

All the experiments involving in human specimens and animals were in accordance with the ethical code and recommendation issued by Ethics Committee of Human Experimentation and Chinese Animal Community and with the Helsinki Declaration of 1975, as revised in 2008.

Consent for publication

Not applicable.

Availability of data and materials

The datasets supporting the conclusions of this article are included within the article and its additional files.

Competing interests

The authors declare that they have no competing interests.

Authors' contributions

All authors meet the authorship requirements. Conception and design: XS, JZ and AL. Development of methodology: XS, HG and YZ. Acquisition of data (provided animals, acquired and managed patients, provided facilities, etc.): HG, YZ and ZX. Analysis and interpretation of data (e.g., statistical analysis, biostatistics, computational analysis): XS, HG and WF. Writing, review, and/or revision of the manuscript: XS, JZ and AL. Administrative, technical, or material support (i.e., reporting or organizing data, constructing databases): YM, WF and AL. Study supervision: WL, YZ. Revision director: JZ. All authors read and approved the final manuscript.

Funding

This study was supported by National Natural Science Foundation of China (81871933, 81802326).

The funders of this project had no role in the design of the study and collection, analysis, and interpretation of data and in writing the manuscript.

Acknowledgments

This study was supported by National Natural Science Foundation of China (81871933, 81802326).

References

1. Siegel RL, Miller KD, Jemal A. Cancer statistics, 2019. Ca-a Cancer Journal for Clinicians. 2019;69(1):7–34.
2. Schmoll HJ, Van Cutsem E, Stein A, et al. ESMO Consensus Guidelines for management of patients with colon and rectal cancer. A personalized approach to clinical decision making. Ann Oncol. 2012;23(10):2479–516.
3. Vogel A, Hofheinz RD, Kubicka S, et al. Treatment decisions in metastatic colorectal cancer - Beyond first and second line combination therapies. Cancer Treatment Reviews. 2017;5954–60.
4. Batlle E, Clevers H. Cancer stem cells revisited. Nat Med. 2017;23(10):1124–34.
5. Fakih MG. Metastatic Colorectal Cancer: Current State and Future Directions. J Clin Oncol. 2015;33(16):1809-+.
6. Vlachogiannis G, Hedayat S, Vatsiou A, et al. Patient-derived organoids model treatment response of metastatic gastrointestinal cancers. Science. 2018;359(6378):920-+.
7. Spence JR, Mayhew CN, Rankin SA, et al. Directed differentiation of human pluripotent stem cells into intestinal tissue in vitro. Nature. 2011;470(7332):105-U20.
8. Simian M, Bissell MJ. Organoids. A historical perspective of thinking in three dimensions. J Cell Biol. 2017;216(1):31–40.
9. Nanki K, Toshimitsu K, Takano A, et al. Divergent Routes toward Wnt and R-spondin Niche Independency during Human Gastric Carcinogenesis. Cell. 2018;174(4):856-+.
10. van de Wetering M, Francies HE, Francis JM, et al. Prospective Derivation of a Living Organoid Biobank of Colorectal Cancer Patients. Cell. 2015;161(4):933–45.
11. Boj SF, Hwang CI, Baker LA, et al. Organoid Models of Human and Mouse Ductal Pancreatic Cancer. Cell. 2015;160(1–2):324–38.
12. Sachs N, de Ligt J, Kopper O, et al. A Living Biobank of Breast Cancer Organoids Captures Disease Heterogeneity. Cell. 2018;172(1–2):373-+.
13. Kopper O, de Witte CJ, Lohmussaar K, et al. An Organoid Platform for Ovarian Cancer Captures Intra- and Interpatient Heterogeneity. Int J Gynecol Cancer. 2019;29A:132-A3.
14. Tuveson D, Clevers H. Cancer modeling meets human organoid technology. Science. 2019;364(6444):952–5.
15. Farrugia MK, Vanderbilt DB, Salkeni MA, et al. Kruppel-like Pluripotency Factors as Modulators of Cancer Cell Therapeutic Responses. Can Res. 2016;76(7):1677–82.
16. Dong Z, Yang L, Lai D. KLF5 strengthens drug resistance of ovarian cancer stem-like cells by regulating survivin expression. Cell Prolif. 2013;46(4):425–35.

17. Nakaya T, Ogawa S, Manabe I, et al. KLF5 Regulates the Integrity and Oncogenicity of Intestinal Stem Cells. Can Res. 2014;74(10):2882–91.
18. Sabando AR, Wang C, He YJ, et al. ML264, A Novel Small-Molecule Compound That Potently Inhibits Growth of Colorectal Cancer. Mol Cancer Ther. 2016;15(1):72–83.
19. Zhao JK, Ou BC, Han DP, et al. Tumor-derived CXCL5 promotes human colorectal cancer metastasis through activation of the ERK/Elk-1/Snail and AKT/GSK3 beta/beta-catenin pathways. Molecular Cancer. 2017;16.
20. Feng HR, Cheng X, Kuang J, et al. Apatinib-induced protective autophagy and apoptosis through the AKT-mTOR pathway in anaplastic thyroid cancer. Cell Death & Disease. 2018;9.
21. Kondo J, Endo H, Okuyama H, et al. Retaining Cell-Cell Contact Enables Preparation and Culture of Spheroids Composed of Pure Primary Cancer Cells From Colorectal Cancer. Gastroenterology. 2011;140(5):339-S.
22. Garnett MJ, Edelman EJ, Heidorn SJ, et al. Systematic identification of genomic markers of drug sensitivity in cancer cells. Nature. 2012;483(7391):570-U87.
23. Xu ZQ, Zhu CC, Chen C, et al. CCL19 suppresses angiogenesis through promoting miR-206 and inhibiting Met/ERK/Elk-1/HIF-1 alpha/VEGF-A pathway in colorectal cancer. Cell Death & Disease. 2018;9.
24. Ou BC, Sun HZ, Zhao JK, et al. Polo-like kinase 3 inhibits glucose metabolism in colorectal cancer by targeting HSP90/STAT3/HK2 signaling. Journal of Experimental & Clinical Cancer Research. 2019;38(1).
25. Ou BC, Cheng X, Xu ZQ, et al. A positive feedback loop of beta-catenin/CCR2 axis promotes regorafenib resistance in colorectal cancer. Cell Death & Disease. 2019;10.
26. Ooft SN, Weeber F, Dijkstra KK, et al. Patient-derived organoids can predict response to chemotherapy in metastatic colorectal cancer patients. Science Translational Medicine. 2019;11(513).
27. Ganesh K, Basnet H, Kaygusuz Y, et al. L1CAM defines the regenerative origin of metastasis initiating cells in colorectal cancer. Can Res. 2020;80(11):40-.
28. Crespo M, Vilar E, Tsai SY, et al. Colonic organoids derived from human induced pluripotent stem cells for modeling colorectal cancer and drug testing (vol 23, pg 878, 2017). Nat Med. 2018;24(4):526-.
29. Gaur S, Chen LL, Ann V, et al. Dovitinib synergizes with oxaliplatin in suppressing cell proliferation and inducing apoptosis in colorectal cancer cells regardless of RAS-RAF mutation status. Molecular Cancer. 2014;13.
30. Hayward RL, Macpherson JS, Cummings J, et al. Enhanced oxaliplatin-induced apoptosis following antisense Bcl-xl down-regulation is p53 and Bax dependent: Genetic evidence for specificity of the antisense effect. Mol Cancer Ther. 2004;3(2):169–78.
31. Yamamoto M, Jin C, Hata T, et al. MUC1-C Integrates Chromatin Remodeling and PARP1 Activity in the DNA Damage Response of Triple-Negative Breast Cancer Cells. Can Res. 2019;79(8):2031–41.

32. Phatak P, Byrnes KA, Mansour D, et al. Overexpression of miR-214-3p in esophageal squamous cancer cells enhances sensitivity to cisplatin by targeting survivin directly and indirectly through CUG-BP1. Oncogene. 2016;35(16):2087–97.
33. Moro H, Hattori N, Nakamura Y, et al. Epigenetic priming sensitizes gastric cancer cells to irinotecan and cisplatin by restoring multiple pathways (vol 12, pg 289, 2019). Gastric Cancer. 2020;23(1):116–7.
34. Hsu HY, Lin TY, Hu CH, et al. Fucoidan upregulates TLR4/CHOP-mediated caspase-3 and PARP activation to enhance cisplatin-induced cytotoxicity in human lung cancer cells. Cancer Letters. 2018;432112–20.
35. Zhao CH, Li YT, Qiu W, et al. C5a induces A549 cell proliferation of non-small cell lung cancer via GDF15 gene activation mediated by GCN5-dependent KLF5 acetylation. Oncogene. 2018;37(35):4821–37.
36. Grothey A, Sargent D, Goldberg RM, et al. Survival of patients with advanced colorectal cancer improves with the availability of fluorouracil-leucovorin, irinotecan, and oxaliplatin in the course of treatment. J Clin Oncol. 2004;22(7):1209–14.
37. Prigerson HG, Bao YH, Shah MA, et al. Chemotherapy Use, Performance Status, and Quality of Life at the End of Life. Jama Oncology. 2015;1(6):778–84.
38. McQuade RM, Stojanovska V, Bornstein JC, et al. Colorectal Cancer Chemotherapy: The Evolution of Treatment and New Approaches. Curr Med Chem. 2017;24(15):1537–57.
39. Pasch CA, Favreau PF, Yueh AE, et al. Patient-Derived Cancer Organoid Cultures to Predict Sensitivity to Chemotherapy and Radiation. Clin Cancer Res. 2019;25(17):5376–87.
40. Drost J, Clevers H. Organoids in cancer research. Nat Rev Cancer. 2018;18(7):407–18.
41. Kondo J, Inoue M. Application of Cancer Organoid Model for Drug Screening and Personalized Therapy. Cells. 2019;8(5).
42. Es HA, Montazeri L, Aref AR, et al. Personalized Cancer Medicine: An Organoid Approach. Trends Biotechnol. 2018;36(4):358–71.
43. Rasmussen MH, Lyskjaer I, Jersie-Christensen RR, et al. miR-625-3p regulates oxaliplatin resistance by targeting MAP2K6-p38 signalling in human colorectal adenocarcinoma cells. Nature Communications. 2016;7.
44. Mohammad RM, Muqbil I, Lowe L, et al. Broad targeting of resistance to apoptosis in cancer. Semin Cancer Biol. 2015;35:78–103.

Tables

Table 1 Clinical characteristics of PDOs donor.

Sample ID	Patient age	Patient sex	Tumor location	TNM stage	PDOs		
					Formation	Growth	Drug
P1	79	M	D	IIA	Yes	Yes	Yes
P2	76	F	R	IIIB	Yes	Yes	Yes
P3	83	M	R	IIA	No	No	No
P4	58	F	R	IV	Yes	Yes	Yes
P5	33	M	S	IIIB	Yes	Yes	No
P6	57	M	T	IV	Yes	Yes	Yes
P7	66	F	R	IIIB	Yes	Yes	Yes
P8	66	M	R	IIIB	Yes	No	No
P9	57	M	S	IIIC	Yes	Yes	No
P10	72	M	D	IIA	Yes	Yes	No
P11	65	M	R	IIIB	Yes	Yes	Yes
P12	72	M	S	IIIB	Yes	No	No

Tumor location: A, ascending colon; T, transverse colon; D, descending colon; S, sigmoid colon, R, rectum.

Figures

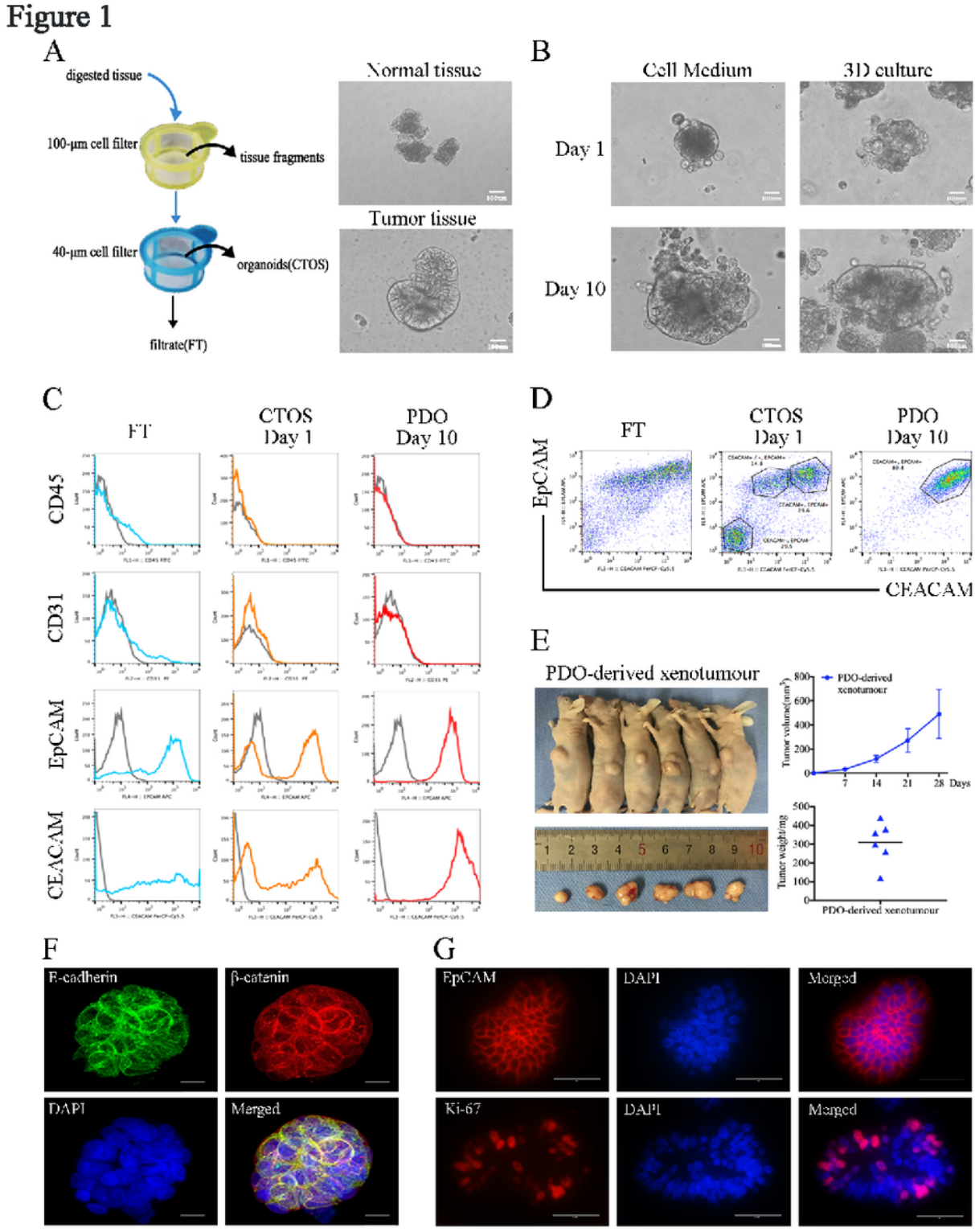

Figure 1

Generation of patient-derived organoids from colorectal cancer. (A) Schematic diagram for the preparation of CRC PDOs. Only tumor samples can form PDOs and normal cells died in a short time. (B) The appearance of CRC PDO in suspension culture or 3D culture. (C&D) Flow cytometry showed that the CRC PDOs were highly purified cancer cell clusters. (E) PDOs can form tumors in nude mice. (F) E-

cadherin(green) and β-catenin(red) staining of PDOs. E-cadherin was located on the cell membrane and linked to β-catenin. (G) PDOs expressed EpCAM and Ki-67. Data represent the mean ± SD.

Figure 2

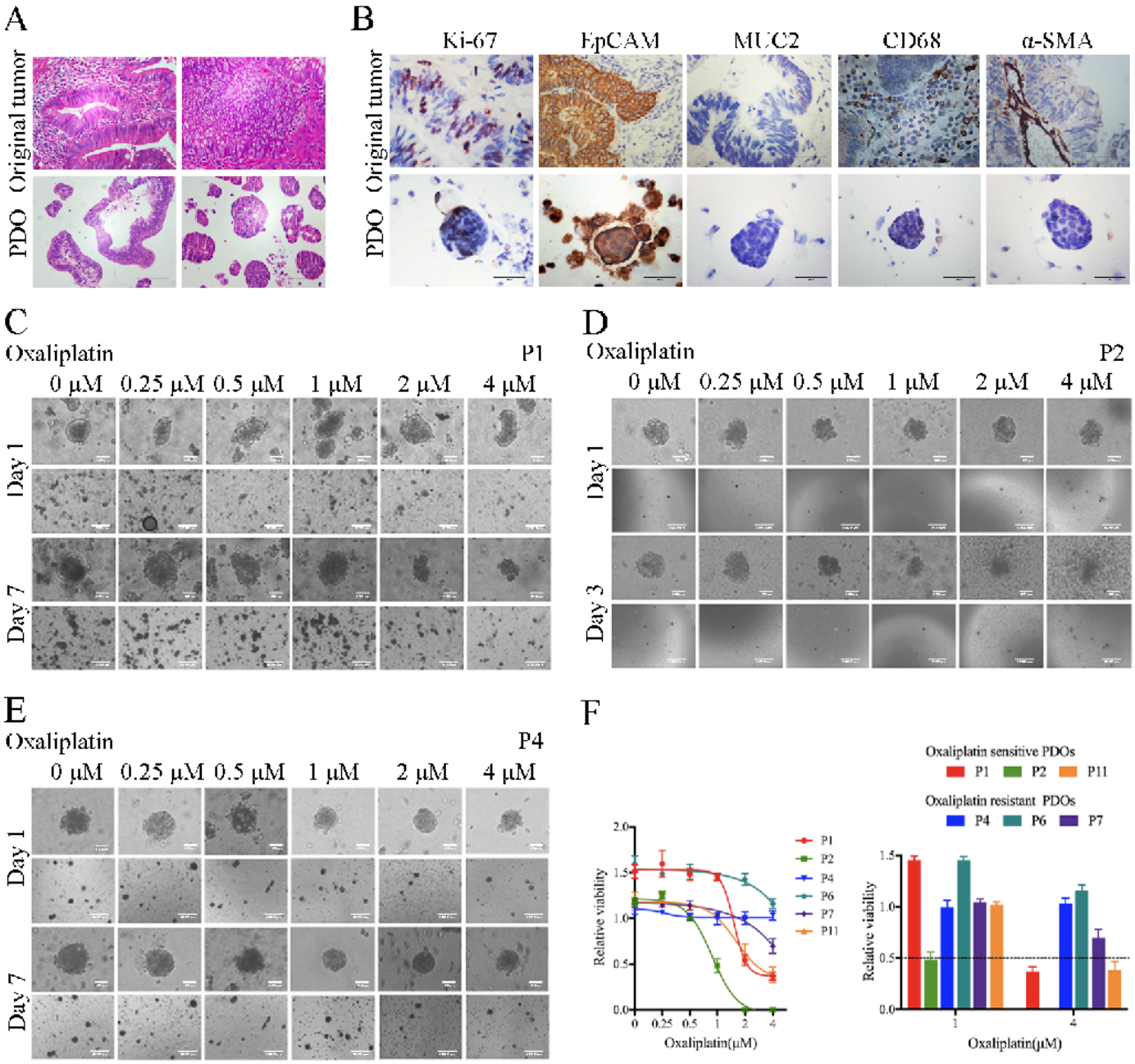

Figure 2

PDOs retained the characteristics of the original tumors. (A) H&E staining showed the internal structure of PDOs and original tumors. (B) The expression of Ki-67, EpCAM, MUC2, α-SMA and CD68 in CRC PDOs and matched original tumors. (C) The results of oxaliplatin sensitivity assays of P1, which was moderately sensitive to oxaliplatin. (D) The results of oxaliplatin sensitivity assays of P2, which was highly sensitive to oxaliplatin. (E) The results of oxaliplatin sensitivity assays of P4, which was resistant to oxaliplatin. (F) The dose-response curves of oxaliplatin. Data represent the mean ± SD.

Figure 3

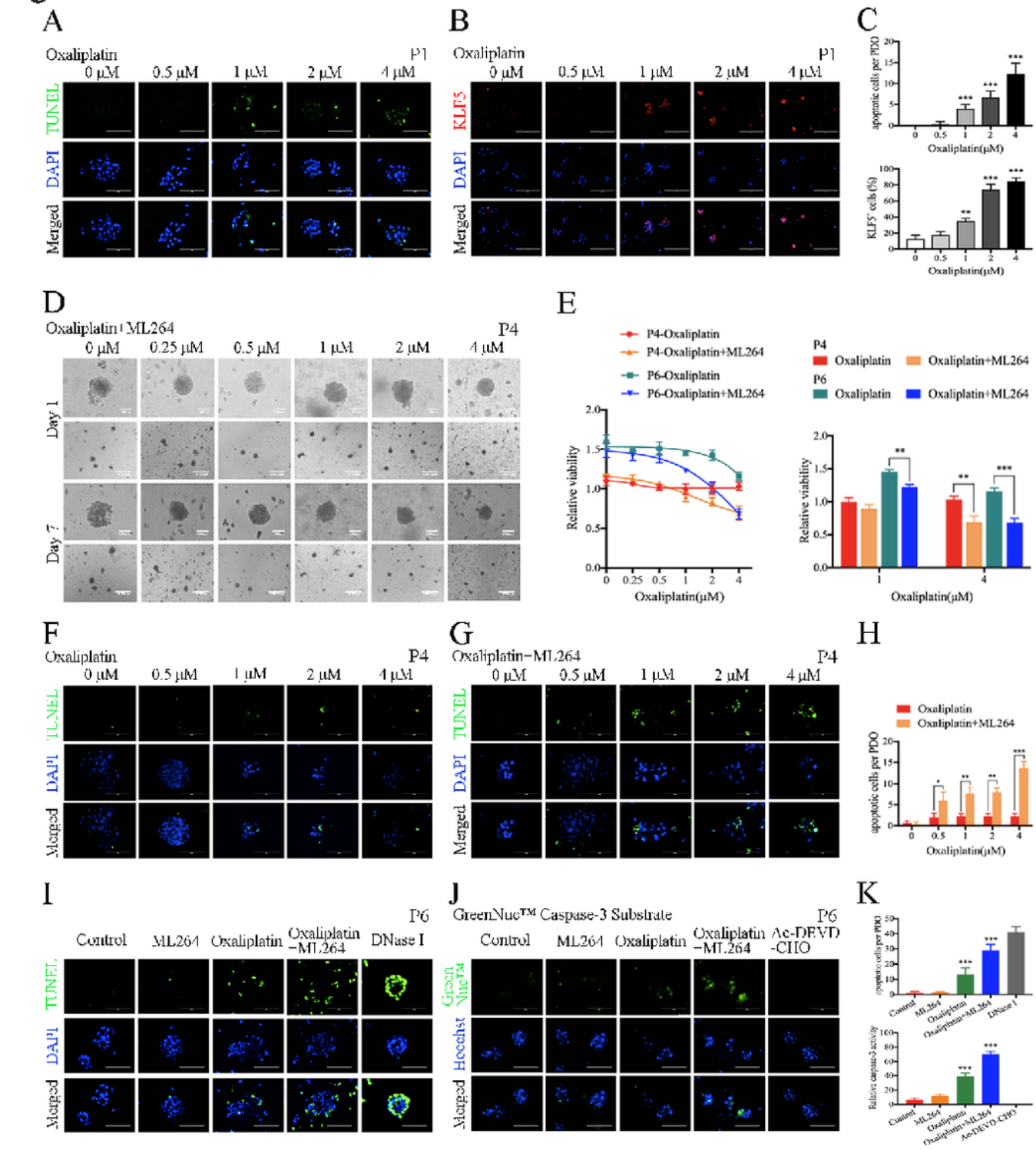

Figure 3

ML264 restored Oxaliplatin sensitivity in CRC PDOs by restoring the apoptotic response. (A) Images of TUNEL(green) apoptosis detection in PDOs treated with Oxaliplatin. (B) KLF5 (red) staining of PDOs treated with Oxaliplatin at indicated concentrations. (C) Oxaliplatin significantly induced apoptosis in a dose-dependent manner. The proportion of KLF5+ cells increased significantly as the dose of oxaliplatin treatment increased. (D)The results of oxaliplatin sensitivity assays of P4 treated with oxaliplatin with a

combination with ML264. (E) The dose-response curves of combined treatment of ML264 and Oxaliplatin. ML264 reduced the dose of Oxaliplatin required to inhibit the growth of PDOs. (F&G&H) Images of TUNEL(green) apoptosis detection in P4 treated with Oxaliplatin at indicated concentrations with or without a combination withML264. ML264 reduced the dose of Oxaliplatin required to induce the apoptotic response of PDOs. (I) Images of TUNEL(green) apoptosis detection in P6 treated with Oxaliplatin with or without a combination with ML264. Dnase was used as a positive control. (J) The activity of caspase 3(green) detection of P6. Ac-DEVD-CHO was used as a negative control. (K) ML264 restored Oxaliplatin-induced apoptotic response and activited of caspase 3. Data represent the mean ± SD. **P < 0.05, **P < 0.01, ***P < 0.001.

Figure 4

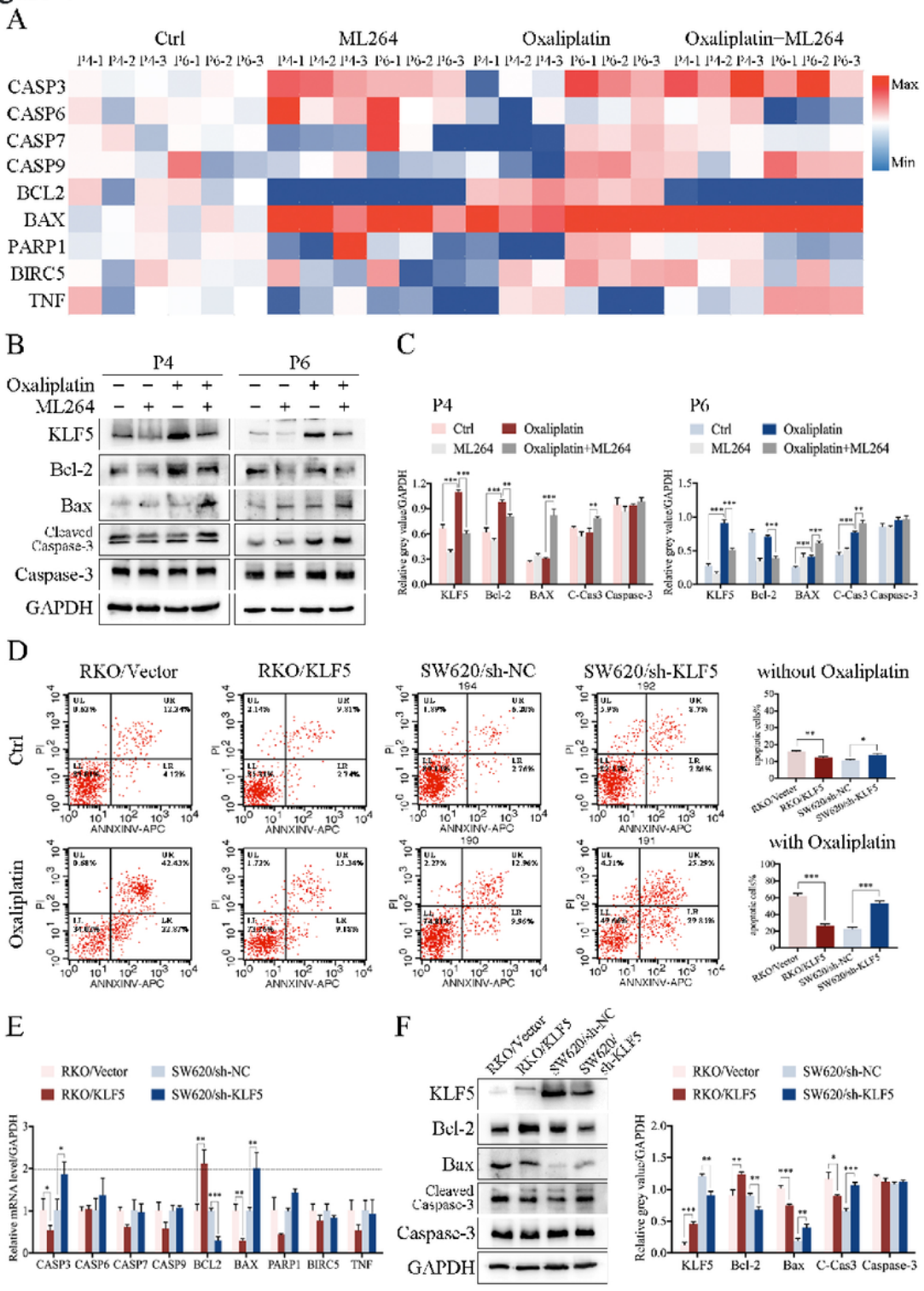

Figure 4

Oxaliplatin induced the expression of KLF5 and a variety of apoptosis-related proteins. (A) qPCR showed the expression of apoptosis-related genes of PDOs treated with Oxaliplatin with or without a combination with ML264. (B) Western blotting of KLF5, Bcl-2, Bax, cleaved caspase 3 and caspase 3 in PDOs. (C) Oxaliplatin induced the expression of KLF5, Bcl-2 and Bax. Oxaliplatin combined with ML264 induced the expression of Bax and Cleaved Caspase-3 and inhibited the expression of KLF5 and Bcl-2. (D) Apoptosis

detection showed that KLF5 promoted apoptosis in CRC cell lines with or without oxaliplatin treated. (E) The expression of apoptosis-related genes of CRC cell lines. (F) Western blotting of KLF5, Bcl-2, Bax, cleaved caspase 3 and caspase 3 in CRC cell lines. KLF5 promoted the expression of Bcl-2 and inhibited the expression of Bax and Cleaved Caspase-3. Data represent the mean ± SD. **P < 0.05, **P < 0.01, ***P < 0.001.

Figure 5

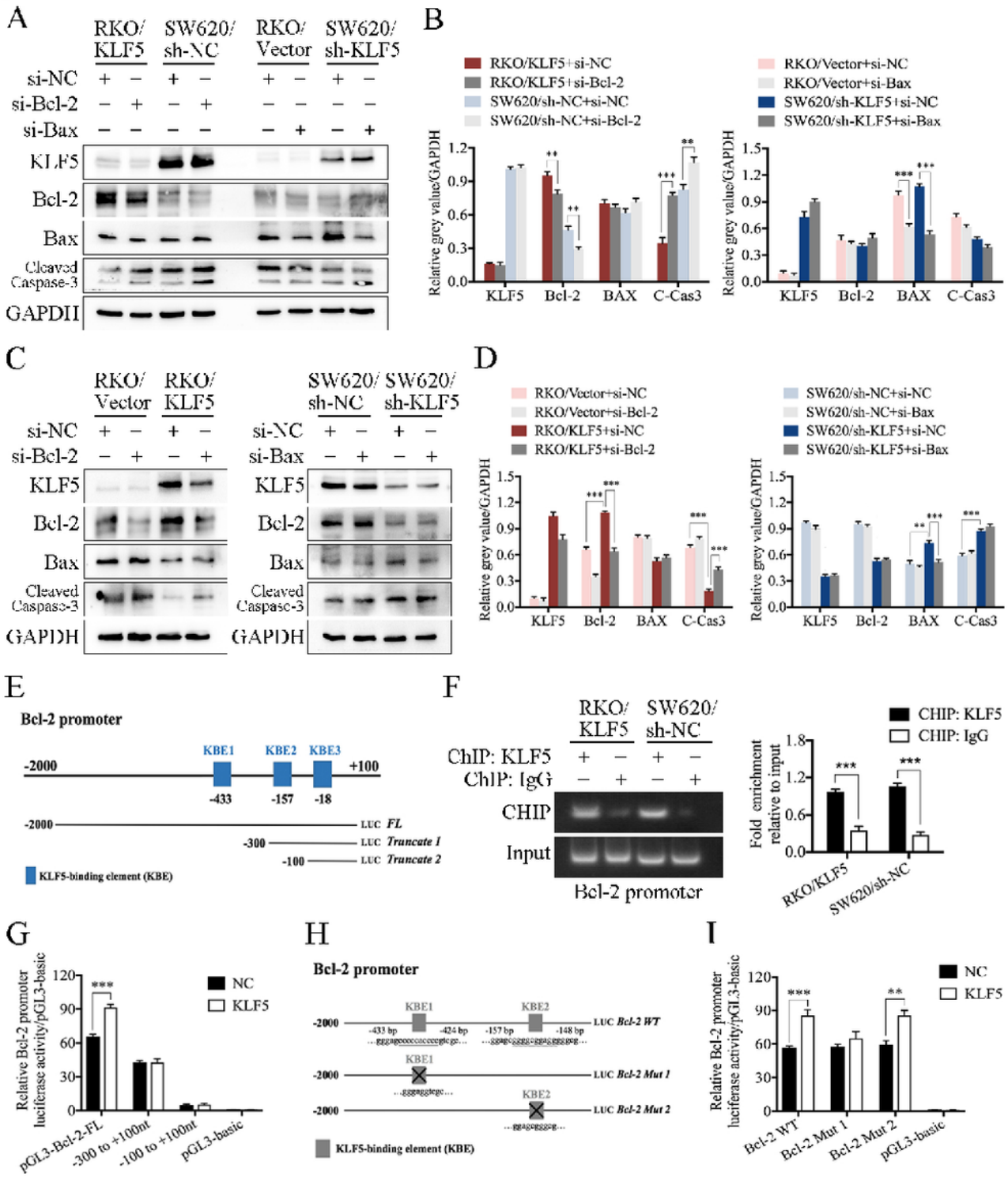

Figure 5

The KLF5/Bcl-2/caspase3 signal pathway affects oxaliplatin-induced apoptosis of CRC cells. (A) Western blotting of KLF5, Bcl-2, Bax, cleaved caspase 3 in CRC cell lines. (B) Knocking down Bcl-2 significantly promoted the expression of Cleaved Caspase-3, whereas knocking down Bax did not affect the expression of Bcl-2 or Cleaved Caspase-3. (C&D) Western blotting showed that inhibiting Bcl-2 can reverse the function of KLF5 of suppressing the expression of Cleaved Caspase-3, whereas inhibiting Bax cannot reverse the function of KLF5 in Cleaved Caspase-3 suppression. (E) KLF5-binding elements (KBE1 to KBE3) on Bcl-2 promoter region. (F) Chromatin immunoprecipitation (ChIP) verified the direct binding of KLF5 to the predicted site(KBE1) of the Bcl-2 promoter. (G) The results of luciferase reporter assay showed that KLF5 only promoted the luciferase activity of pGL3-Bcl2-FL. (H) Schematic diagram showed the mutation site of Bcl-2 Mut 1 and Bcl-2 Mut 2 plasmids. (I) The results of luciferase reporter assay showed that KLF5 can not promoted the luciferase activity of Bcl-2 Mut 1, which did not contain KBE1 sequence. Data represent the mean ± SD. **P < 0.05, **P < 0.01, ***P < 0.001.

Figure 6

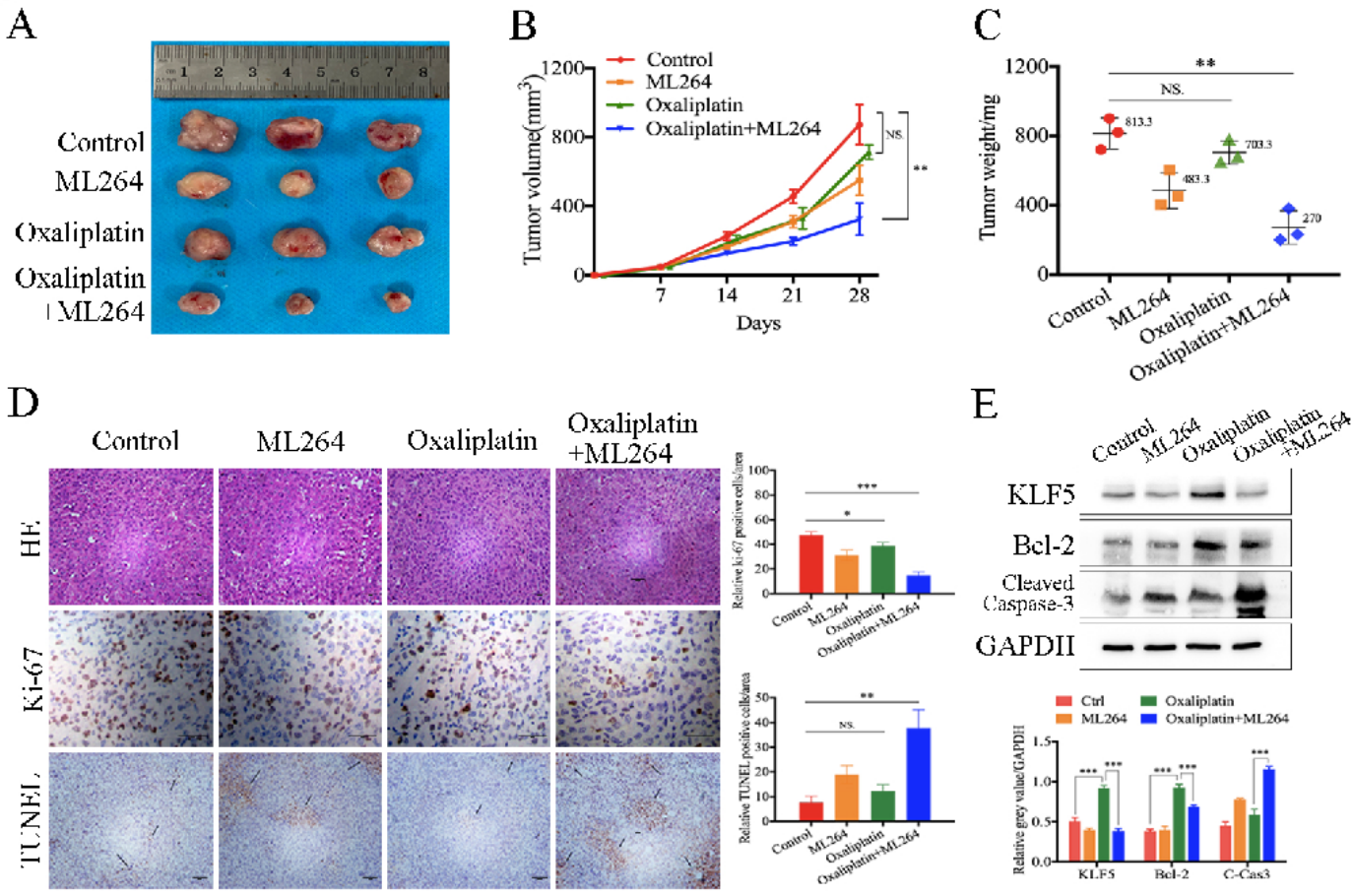

Figure 6

Inhibition of KLF5 overcomes oxaliplatin resistance in xenograft tumors. (A&B) Nude mice were injected s.c. with PDOs. After tumor diameter reached ~ 5mm, mice were treated with oxaliplatin alone or in combination withML264 as indicated. Tumor volume at indicated time points was calculated and plotted (n=3 in each group). (C) The combined use of ML264 can significantly inhibit tumor growth in xenograft tumors derived from Oxaliplatin-resistant PDOs. (D) TUNEL and ki-67 immunostaining were used to

analyzed the apoptosis level of xenograft tumors. Arrows indicate example cells with positive staining. ML264 significantly restored the oxaliplatin-induced tumor apoptosis. (E) Western blotting was used to analysis KLF5, Bcl-2 and Cleaved Caspase-3. Data represent the mean ± SD. **P < 0.05, **P < 0.01, ***P < 0.001.

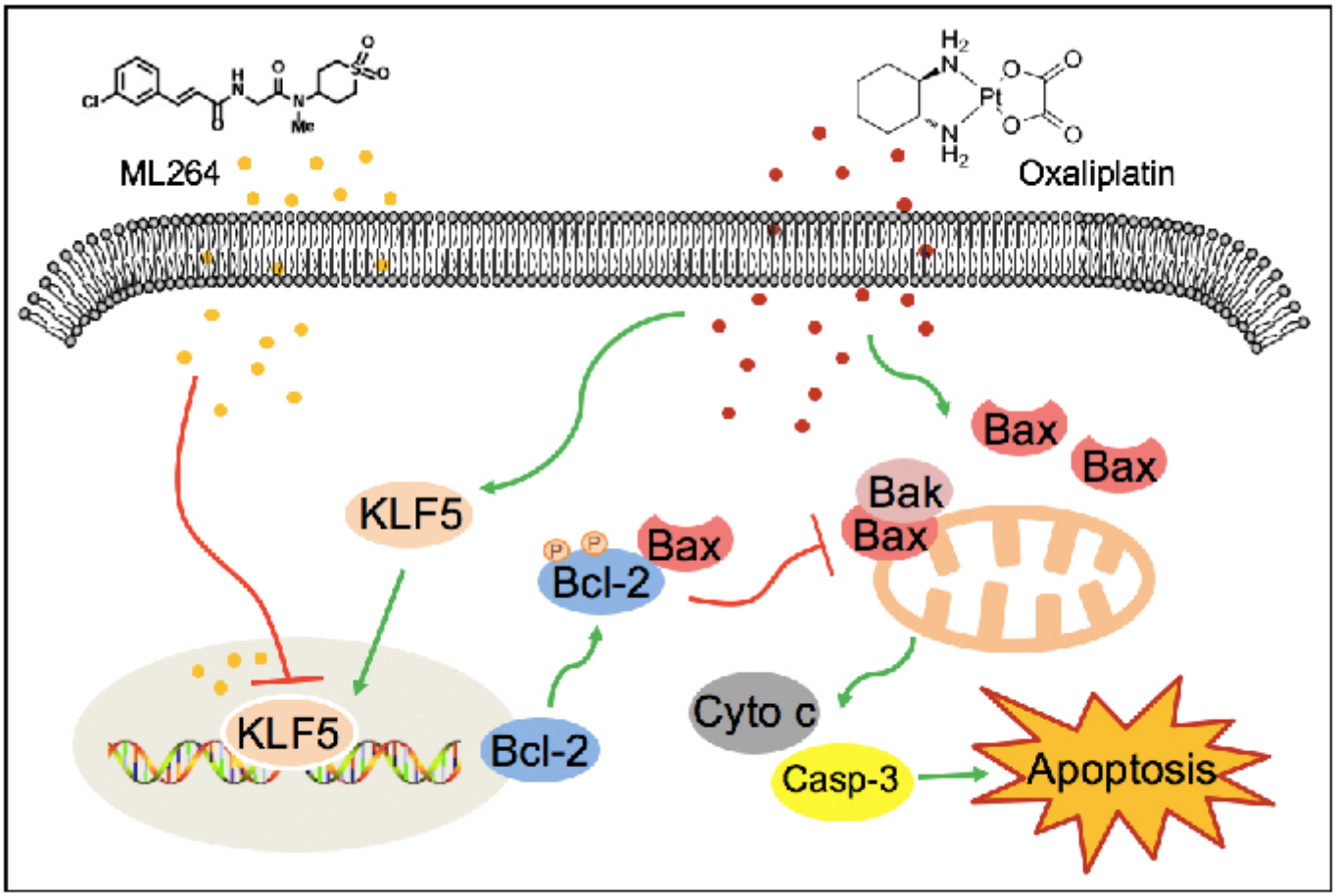

Figure 7

Schematic diagram showes the mechanisms of CRC cells resistance to oxaliplatin and ML264 restores Oxaliplatin sensitivity of colorectal cancer. Overexpression of KLF5 and its downstream anti-apoptotic factor Bcl-2 was one of the mechanisms for CRC to resist oxaliplatin.

Supplementary Files

This is a list of supplementary files associated with this preprint. Click to download.

- supplementarydata.docx